Experimental Study of the Scattering of Acoustic Energy from Solid Metal Spheres in Water*

L. D. HAMPTON AND C. M. MCKINNEY

Defense Research Laboratory, The University of Texas, Austin, Texas

(Received December 27, 1960)

An experimental study of the scattering of acoustic energy from solid metal spheres in water has been carried out in the frequency range 50–150 kc and with a range of sphere sizes from 1 to 7 in. in diam, giving values of ka (acoustic radius) from 4.1 to 57. Data are presented which show the scattered pulse formation for pulses which are short compared to the sphere and for pulses which are long compared to the sphere as a function of frequency, of scattering angle, and of sphere composition. The study shows that the spheres cannot be treated as rigid bodies since an appreciable amount of energy penetrates the surface and results in a complicated echo structure for the scattered signal. The back-scattered target strength of spheres for short pulses (and considering only the surface-reflected pulse) is essentially constant with frequency for large ka, and is slightly less than the theoretical value for rigid spheres. For pulses which are long compared to the transit time across the sphere, the target strength fluctuates as much as 30 db for small changes in frequency. For short pulses the angular distribution of the scattered energy is fairly uniform over the back 180°, but this is not true for long pulses.

INTRODUCTION

THE problem of the disturbance of plane waves of sound when they impinge on a rigid and immovable sphere has been studied by a number of investigators. Lord Rayleigh[1] proposed a solution for the limiting case where the sphere is small compared to the wavelength of sound and this type of scattering bears his name. Morse,[2] and later Stenzel,[3] obtained solutions to include the case where the sphere is not necessarily small compared to the wavelength and calculated the predicted distribution in angle of the scattered energy at large distances for spheres of several acoustic radii. Wiener[4–6] carried out extensive theoret-
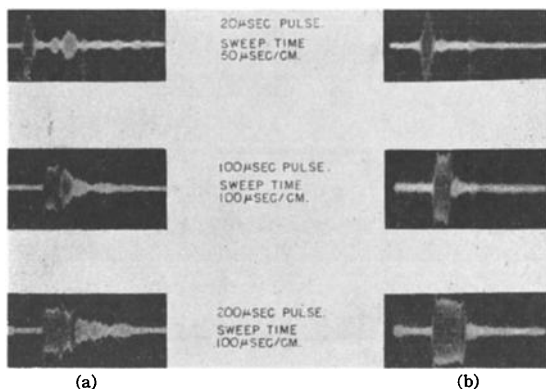

FIG. 1. Oscilloscope photographs of scattered signal at two scattering angles for a 7-in. diam solid aluminum sphere. Frequency: 150 kc; oscilloscope scale in cm. (a) Backscattering; (b) scattering at 250°.
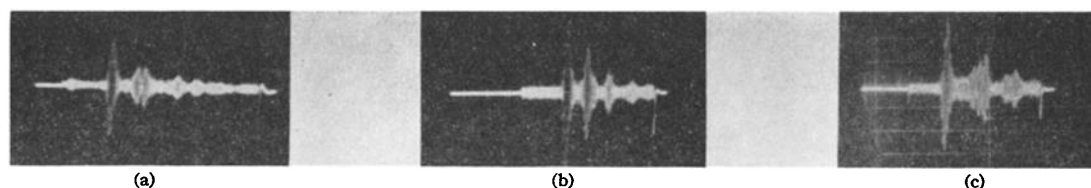
ical and experimental work on the diffraction of various objects, including rigid spheres, and measured the sound field near the surface of "rigid" spheres in air. Anderson. has studied the problem of scattering from fluid spheres[7] Faran[8] expanded the work of Morse to obtain solutions for scattering of sound by spheres and cylinders for the case in which the sound penetrates the scatterer. He tabulated the necessary functions for the case of the cylinders to compare theoretical and experimental values.

It appears that comparatively little experimental work has been done on the problem of sound scattering by spheres and that the bulk of the theoretical work has been for the case of the rigid sphere although in practice one can never achieve this condition. It is the purpose of this paper to describe briefly the results of an experimental study of the scattering of acoustic energy by solid spheres immersed in water. Data are presented which show the distribution in angle of the scattered energy, the back-scattered intensity (target strength) as a function of frequency for both long and short pulses, and the echo structure of the scattered pulses.

EXPERIMENTAL ARRANGEMENT

The measurements were made at the Lake Travis Test Station, operated by Defense Research Laboratory of The University of Texas. The mechanical apparatus for the measurements consisted of a support for the sphere, a support for the sound source, and a rotating boom supporting the hydrophone. The axis of rotation of the hydrophone boom was through the point of suspension of the sphere and both transducers and the sphere were aligned to be in the plane of rotation. The distances of the projector and hydrophone from the sphere were each approximately 10 ft. The hydrophone boom was driven by an electric motor and performed 1 revolution in 10 min.

[1] Lord Rayleigh, *The Theory of Sound* (Dover Publications, New York, 1945), 1st American ed., p. 272.
[2] P. M. Morse, *Vibration and Sound* (McGraw-Hill Book Company, Inc., New York, 1936 and 1948, 2nd ed.), p. 354.
[3] H. Stenzel, Elek. Nachr. Tech. 15, 71 (1938).
[4] F. M. Wiener, J. Acoust. Soc. Am. 19, 444 (1947).
[5] F. M. Wiener, J. Acoust. Soc. Am. 20, 367 (1948).
[6] F. M. Wiener, J. Acoust. Soc. Am. 21, 334 (1949).
[7] V. C. Anderson, J. Acoust. Soc. Am. 22, 426 (1950).
[8] J. J. Faran, Jr., J. Acoust. Soc. Am. 23, 405 (1951).

FIG. 2. Oscilloscope photographs of back-scattered signal from three spheres. Frequency: 120 kc; pulse width: 20 μsec; sweep time: 100 μsec/cm; oscilloscope scale in cm. (a) 7-in. diam Al sphere. (b) 5-in. diam Al sphere. (c) 5-in. diam brass sphere.

The targets used in the study were machined aluminum spheres having diameters of 1, 3, 5, and 7 in. and a brass sphere of 5-in. diameter. The acoustic impedance of aluminum relative to water is approximately 10 while that of brass is approximately 20. The spheres were suspended by slender monofilament nylon. The electronic equipment was of conventional design and a pulse transmission system was used. The pulser was used both to key the carrier and to "gate" the receiver. A prf of 160 per sec permitted an unambiguous maximum range of 15 ft. Pulse widths from 20 to 500 μsec were employed for the various experiments. The frequency range employed was from 50 to 150 kc.

Similar transducers were used for projection and reception, each having an aperture of 7.0 in. and were of the "line-and-cone" type.[9] When these transducers are used, the test distance of 10 ft between transducers and target satisfies the requirement for "far-field" scattering for the range of frequencies employed. The combination of transducer directivity, receiver gating, and vertical location of the transducers (38 ft above the lake bottom and 12 ft below the water surface) eliminated interference due to multiple transmission paths.

Data on echo structure and target strength were recorded by using a Land camera to photograph an oscilloscope display while distribution-in-angle data were recorded on a Brüel and Kjaer level recorder.

EXPERIMENTAL RESULTS

Echo Structure

Figure 1 shows a comparison of the scattered signal for various pulse widths at the backscattering point (hydrophone adjacent to projector) and for a bistatic angle of 110°, which is an angle that corresponds to a peak in the scattered signal. The data were obtained using the 7-in. diam aluminum sphere and a frequency of 150 kc. A polar diagram of the scattered energy for this condition is shown in Fig. 9. In Fig. 1 the first pulse (from left to right) is the surface-reflected pulse and for a pulse length of 20 μsec (corresponding to a range extension of approximately 0.6 in. in water) the surface-reflected pulse for the two hydrophone positions are approximately of equal level but the subsequent pulse structure is decidedly different. For the longer pulse lengths of 100 μsec (approx 3.0-in. range extension in water), interference begins between the different scattered pulses for the backscattered case and for a pulse length of 200 μsec (6-in. range extension) the successive echoes are essentially merged into a long decaying single pulse. However, for the bistatic case, the dominant scattered pulse still appears to be the first surface reflection with negligible contribution from other echoes. The difference may be due to a longitudinal mode of oscillation set up by the incident pulse which would affect the back scattering in a different manner than the bistatic scattering.

Figure 2 shows the backscattered echo structure for the 7-in. diam aluminum sphere, and the 5-in. diam aluminum and brass spheres. Again the successive pulses are evident. The small negative pulses mark the beginning and end of the receiver gate.

The pulse photograph for the 5-in. diam aluminum sphere using a 20-μsec pulse at 120 kc has the correct spacing between pulses (considering a water path) for equatorial and rear surface reflections. However, as a
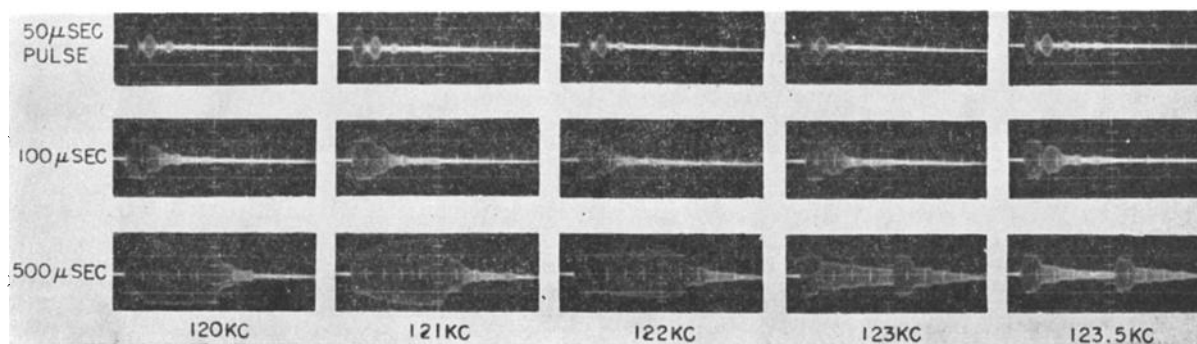

FIG. 3. Back-scattered pulse from a 5-in. diam aluminum sphere; sweep 100 μsec/cm.

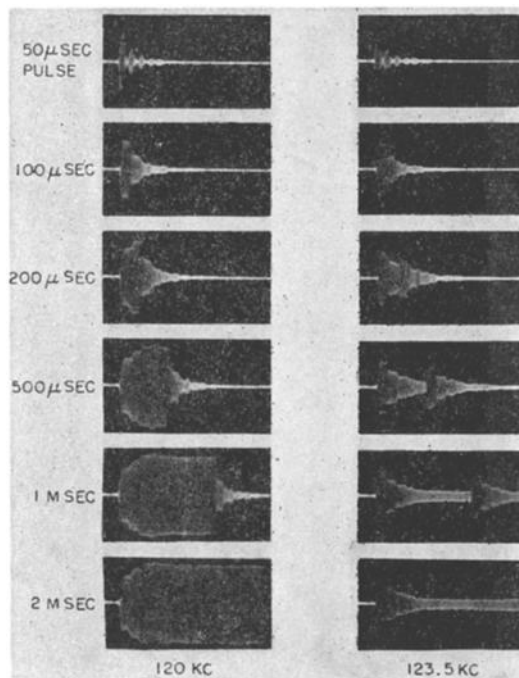[9] R. E. Mueser, J. Acoust. Soc. Am. 19, 952 (1947).

FIG. 4. Back-scattered pulse from a 5-in. diam aluminum sphere; sweep 150 μsec/cm.

comparison with the 5-in. diam brass sphere will show, the spacing depends on the composition of the sphere and thus cannot be attributed to a water path. The pulse photographs for the 7-in. diam aluminum and

the 5-in. diam brass spheres do not show echoes which have a spacing that could be attributed to an equatorial or rear surface echo. If an equatorial or a rear surface reflection is present, the level is far below the level of the front surface reflection and such echoes are also secondary to the reradiation effects exhibited here.

Figure 3 shows the variation in amplitude of the backscattered echo for three pulse lengths as a function of frequency, using the 5-in. diam aluminum sphere. At 120 kc the backscattered echo for the long pulse condition is a maximum and at 123.5 kc the backscattered echo is a minimum as can be seen in Fig. 5. Three intermediate frequencies are shown indicating the transition from maximum to minimum. It is of interest to note that the echo structure using a 50-μsec pulse, which is short enough to resolve the several echoes, remains essentially constant with frequency.

Figure 4 shows more detail of the backscattered echo for the two frequencies of 120 and 123.5 kc and is a direct comparison of the maximum and minimum backscattered echoes as a function of pulse length.

These four figures show that the spheres are not behaving as rigid omnidirectional scatterers but that appreciable energy penetrates the solid, undergoes further reflections, and reradiates at a later time. The condition for a maximum or a minimum in backscattered echo appears to be controlled by the phase relation between surface reflected energy and the energy which is reradiated by the sphere.
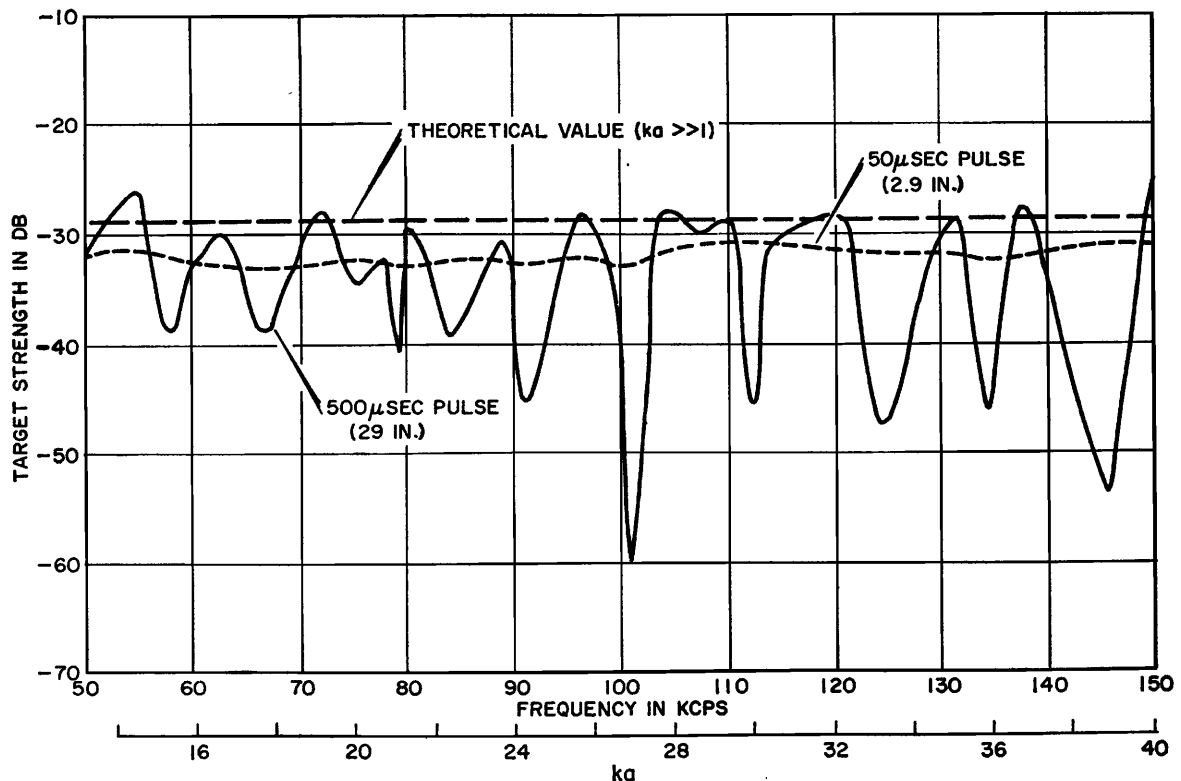

FIG. 5. Measured target strength of a 5-in. diam solid aluminum sphere as a function of frequency for different pulse lengths.
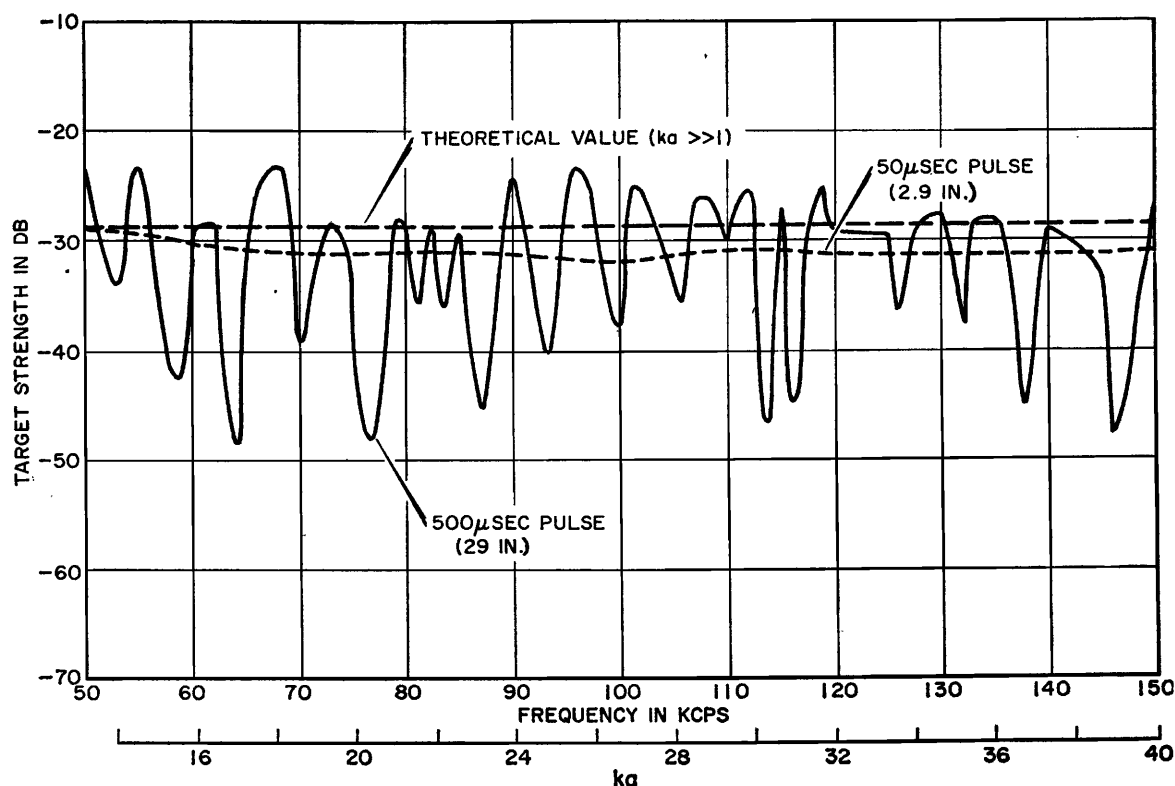
FIG. 6. Measured target strength of a 5-in. diam solid brass sphere as a function
of frequency for different pulse lengths.

Target Strength

In sonar work, target strength is a term used to characterize underwater targets and is defined by

$$T(\text{target strength}) = 10 \log I_r/I_0 \text{ db},$$

where I_r is the intensity of the reflected signal specified 1 yd from the target and I_0 is the intensity of the incident signal. For a rigid sphere that is large compared to the wavelength, the target strength is independent of frequency. Because of the independence of target strength on frequency and orientation, the sphere is often used as a standard reference sonar target. In practice though, one does not have rigid spheres and this results in spheres having a target strength which is usually a function of frequency.

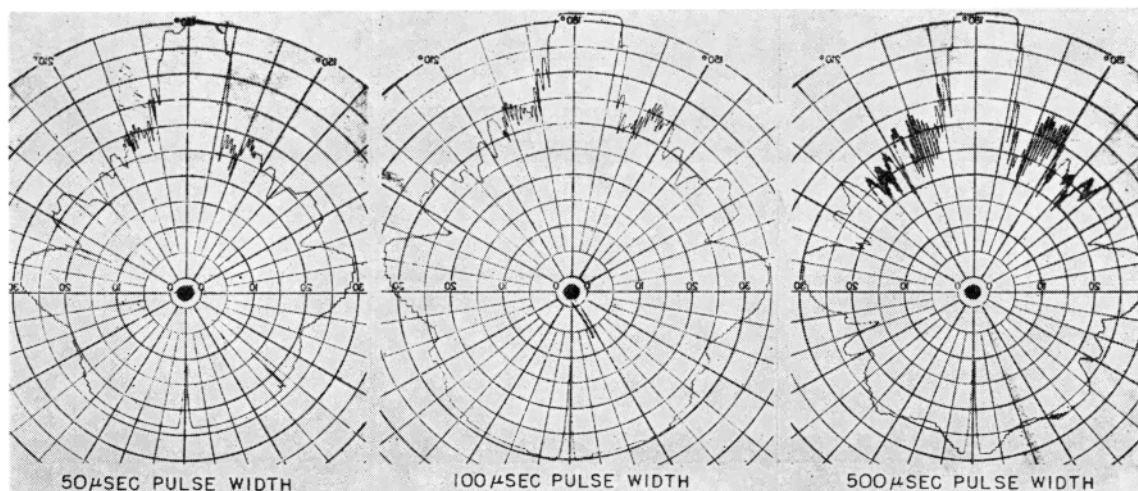Figures 5 and 6 show the measured values of target

FIG. 7. The distribution in angle of acoustic energy scattered from a 5-in. diam solid aluminum sphere as a function of pulse width. Frequency: 120 kc; radial scale: 5 db per division; angular scale 10° per division; sound source at 0°. (The polar diagrams shown in Figs. 7–14 are mirror images of the actual figures. Zero degrees is at the bottom of the figures shown and 180° at the top. The angle increases in the counterclockwise direction and each angular division is 10°.)
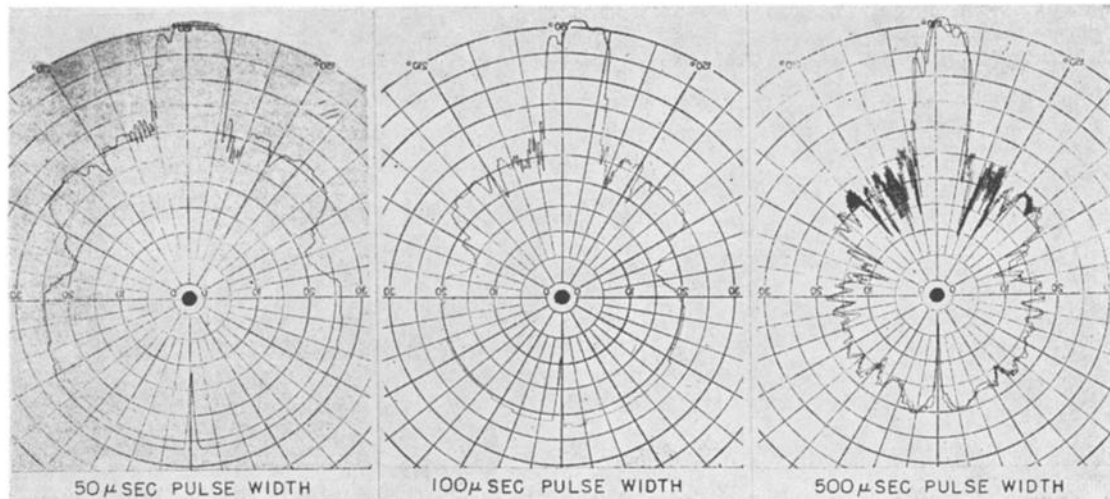
FIG. 8. The distribution in angle of acoustic energy scattered from a 5-in. diam solid brass sphere as a function of pulse width. Frequency: 120 kc; radial scale: 5 db per division; angular scale: 10° per division; sound source at 0°.

strength for the 5-in. diam aluminum and brass spheres, respectively, as compared with the theoretical values for rigid spheres of the same diameter. It can be seen that for the short pulse case in which all of the subsequent pulses were gated out of the receiver, the target strength is relatively constant over a wide range of acoustic radius ka ($k = 2\pi/\lambda$ and a = radius of sphere). The measured value is less than the theoretical value for the rigid sphere and this would be expected since some of the incident energy penetrated the sphere and was not included in the reflected pulse used for these measurements. When a pulse with a range extension much greater than the diameter of the sphere was used, it gave the results shown by the solid curves. Because of constructive and destructive interference between the surface reflected pulse and the successive reradiated pulses, the target strength varies rapidly with frequency, having excursions of as much as 30 db. For the long pulse condition also, it is obvious that the target strength does depend on the composition of the sphere.

As one would expect, the short pulse target strength of brass is closer to the rigid sphere value than for aluminum, since the acoustic impedance of brass is approximately twice that of aluminum. Since the theoretical value for target strength of a rigid sphere assumes perfect reflection, the fact that the value for target strength obtained using a long pulse is often greater than the theoretical value is not readily explained. It indicates that perhaps at those frequencies

additional energy is applied into the sphere over a larger portion of the spherical surface and this energy is reradiated in the backscattering direction in phase with the surface reflection.

The average value of the measured short pulse target strength for all of the spheres as compared to the values for a rigid sphere are shown in Table I. If the value obtained for the 1-in. diam aluminum sphere is neglected since it does not satisfy the condition of a sphere that is large compared to the wavelength, then the average difference between measured target strength and theoretical target strength for aluminum is 2.8 db and for brass 1.9 db. This could be interpreted as a reflection coefficient of 0.52 for aluminum and 0.65 for brass, as compared to a plane wave reflection coefficient for normal incidence on a plane surface of 0.67 for aluminum and 0.82 for brass.

Angular Distribution of Scattered Energy

Figures 7 and 8 are polar diagrams which show the effect of pulse width on the scattered energy from the 5-in. diam aluminum and brass spheres, respectively. The radial scale is logarithmic and each division is 5 db. The direction of the sound source is from 0° on the diagrams and the notch in the patterns at that angle is caused by the hydrophone passing between the projector and sphere and masking the sphere. The 50-μsec pulse has a range resolution of 1.45 in., the 100-μsec pulse a resolution of 2.9 in., and the 500-μsec pulse a resolution of 15 in. In each case the receiver was gated to respond only to the scattering beginning with the initial surface scattering and terminating at the end of the original pulse duration. For the 50-μsec pulse, the diagrams show isotropic behavior through wide angles (approximately 85° for aluminum and 190° for brass). As the pulse is lengthened the isotropic behavior disappears and the scattered energy shows angular dependence.

TABLE I.

Sphere	Measured target strength	Theoretical target strength	Difference
7-in. diam aluminum	−28.1 db	−26 db	−2.1 db
5-in. diam aluminum	−31.9	−28.8	−3.1
5-in. diam brass	−30.7	−28.8	−1.9
3-in. diam aluminum ($ka > 19$)	−36.6	−33.4	−3.2
1-in. diam aluminum ($ka = 6$)	−45.0	−43.5	−1.5

The diagrams for the aluminum sphere exhibit peaks at approximately 100° and 260°, which are characteristic of all of the diagrams for aluminum for $ka > 20$. Similarly, the diagrams for brass exhibit nulls at approximately 100° and 250°, which is also characteristic of patterns for brass for ka from 14 to 41 (the range of measurement). This variation indicates a dependence on metal composition for general scattering even for the short pulse condition. Because these peaks at 100° and 260° for aluminum are the single characteristic which occur on all patterns independent of frequency and pulse length (and similarly, the nulls at 110° and 250° for brass), it appears that the mechanism for this behavior is not the same as that which causes the peaks and nulls in the backscattering level, which did exhibit a marked dependence on frequency and pulse length.

Figure 9 shows the distribution in angle of the scattered energy as measured for the 7-in. diam aluminum sphere using a 500-μsec pulse and frequencies from 150 to 50 kc. This is a range of values of ka from 57 to 19. The patterns were obtained by allowing the boom to rotate once with the sphere centered in the sound field and then allowing the boom to repeat with the sphere

removed from the field but with the nylon support in position.

On each pattern the signal level with the sphere removed is below the zero level of the recorder from the backscattering point to about 120° in each direction. Then the curve begins to describe the smooth minor lobes of the projector beam pattern. These lobes are distorted because of two effects: first, the directivity of the hydrophones reduces the signal level of the lobes since the hydrophone is pointing directly toward the point of rotation rather than toward the projector; and second, the signal is gated in time by the receiver gate. As the boom moves into the line of direct transmission, the signal level increases rapidly due to the main lobe of the projector being directly in line with the main lobe of the hydrophone and also to the coincidence in time of the direct path travel time with the receiver gate width. With the sphere in place, the scattered energy from the sphere varies with angle as shown by the outer trace. This is a relatively smooth curve until the contribution from the direct path becomes significant. As the direct path contribution increases, it causes the received signal to fluctuate due to constructive and
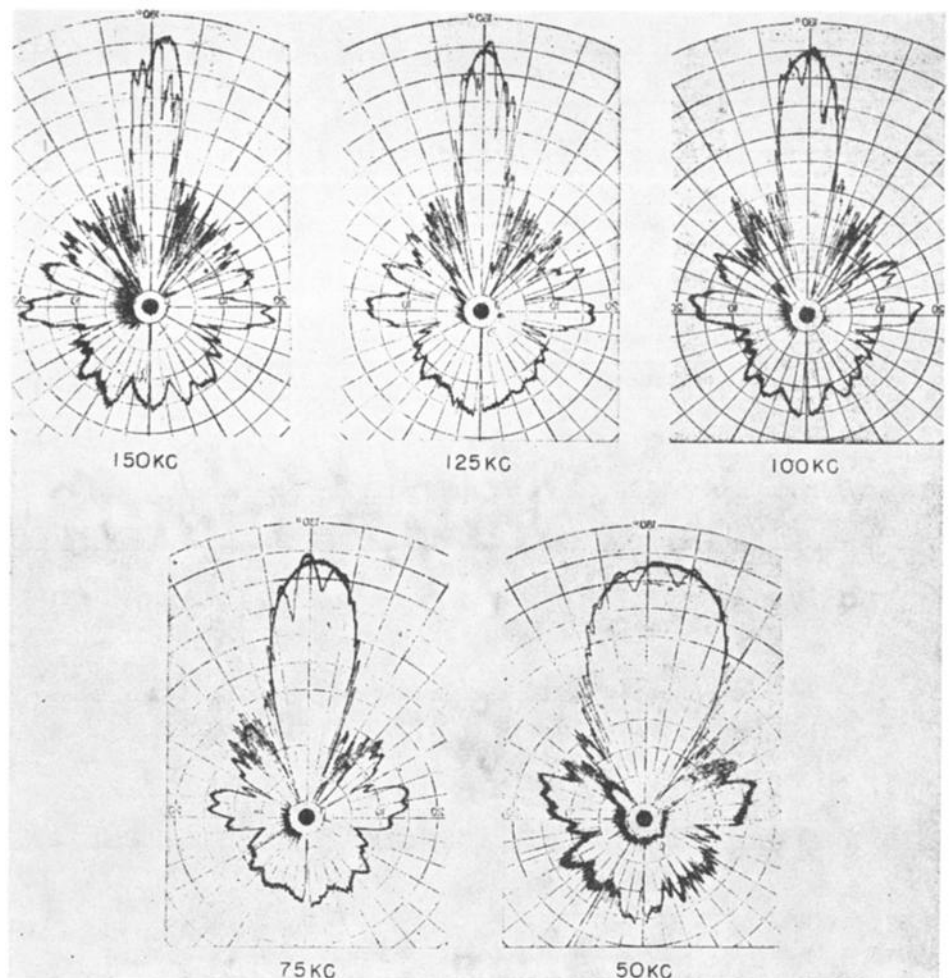

FIG. 9. The distribution in angle of acoustic energy scattered from a 7-in. diam solid aluminum sphere. Pulse length: 500 μsec; radial scale: 5 db per division; angular scale: 10° per division; sound source at 0°.
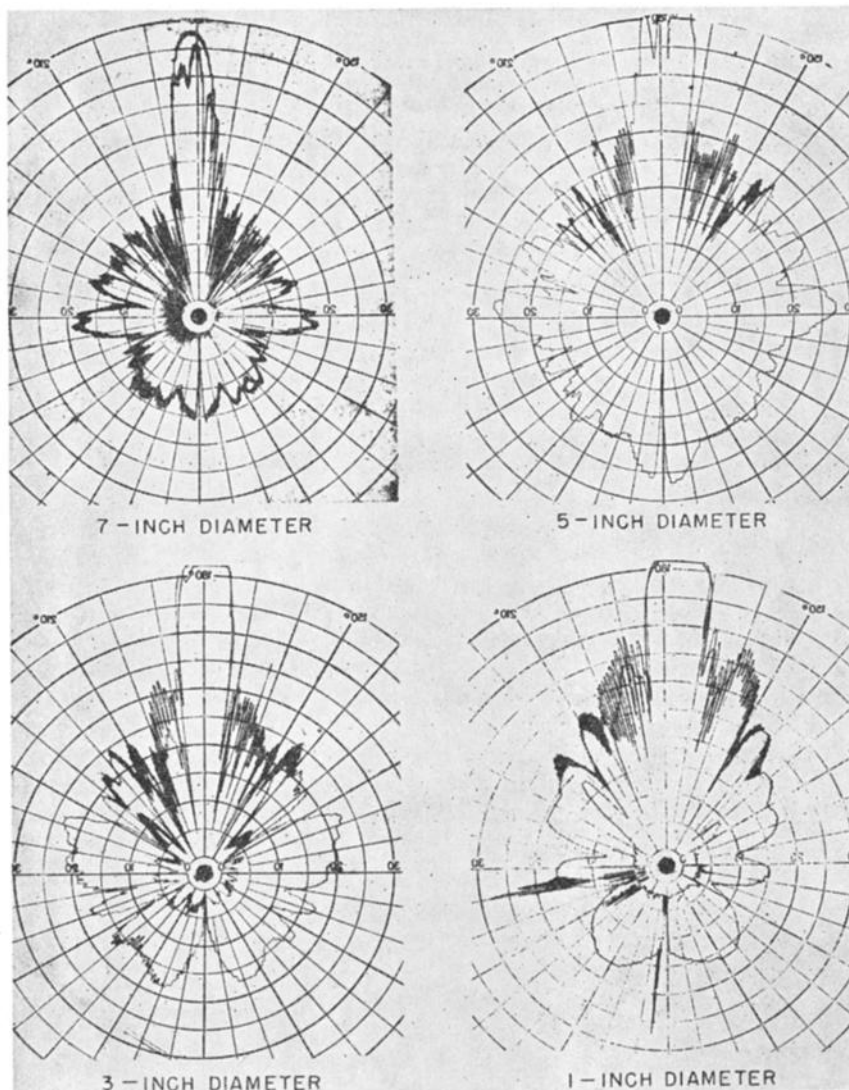
150KC   125KC   100KC

75KC   50KC

FIG. 10. The distribution in angle of acoustic energy scattered from solid aluminum spheres. Frequency: 150 kc; pulse length: 500 μsec; radial scale: 5 db per division, angular scale: 10° per division; sound source at 0°.
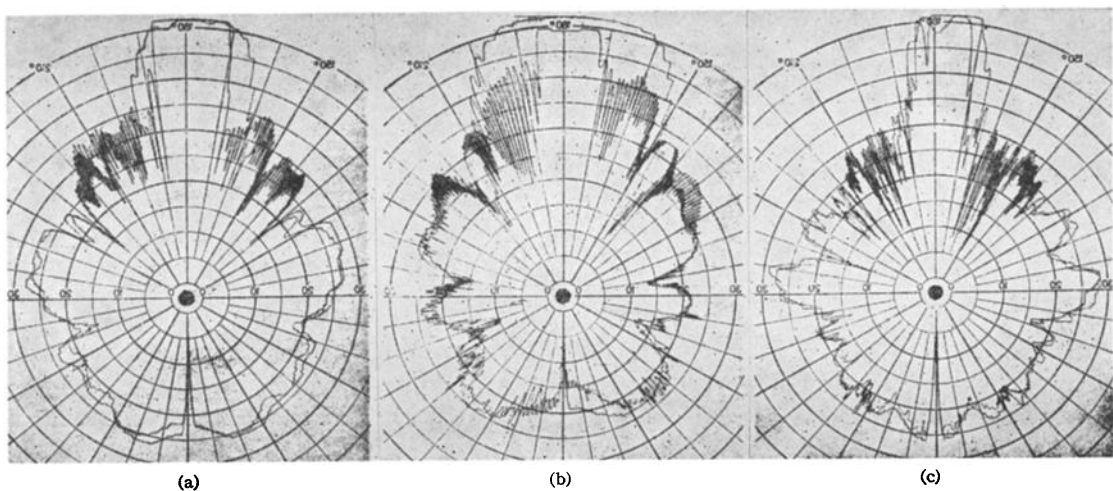
7 - INCH DIAMETER

5 - INCH DIAMETER

3 - INCH DIAMETER

1 - INCH DIAMETER

(a)

(b)

(c)

FIG. 11. The distribution in angle of acoustic energy scattered from different spheres with equal values of *ka*. Pulse length: 500 μsec; 5 db per division; angular scale: 10° per division; sound source at 0°. (a) *ka*=8.2; 1-in. diam Al sphere at 150 kc and a 3-in. diam Al sphere at 50 kc. (b) *ka*=20; 3-in. diam Al sphere at 125 kc and a 5-in. diam Al sphere at 75 kc. (c) *ka*=38; 5-in. diam Al sphere at 140 kc and a 7-in. diam Al sphere at 100 kc.
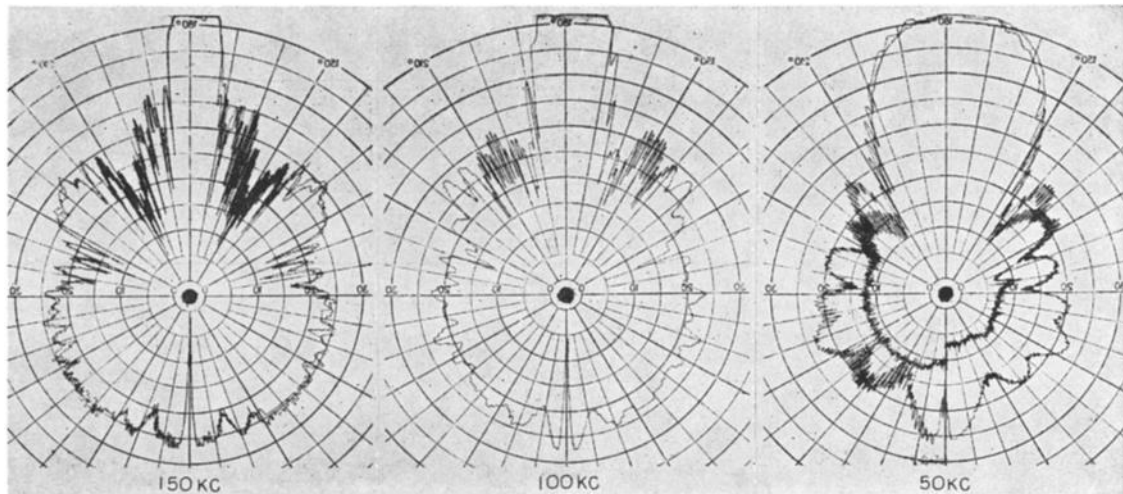
FIG. 12. The distribution in angle of acoustic energy scattered from a 5-in. diam solid brass sphere. Pulse length: 500 μsec; radial scale: 5 db per division; angular scale: 10° per division, sound source at 0°.
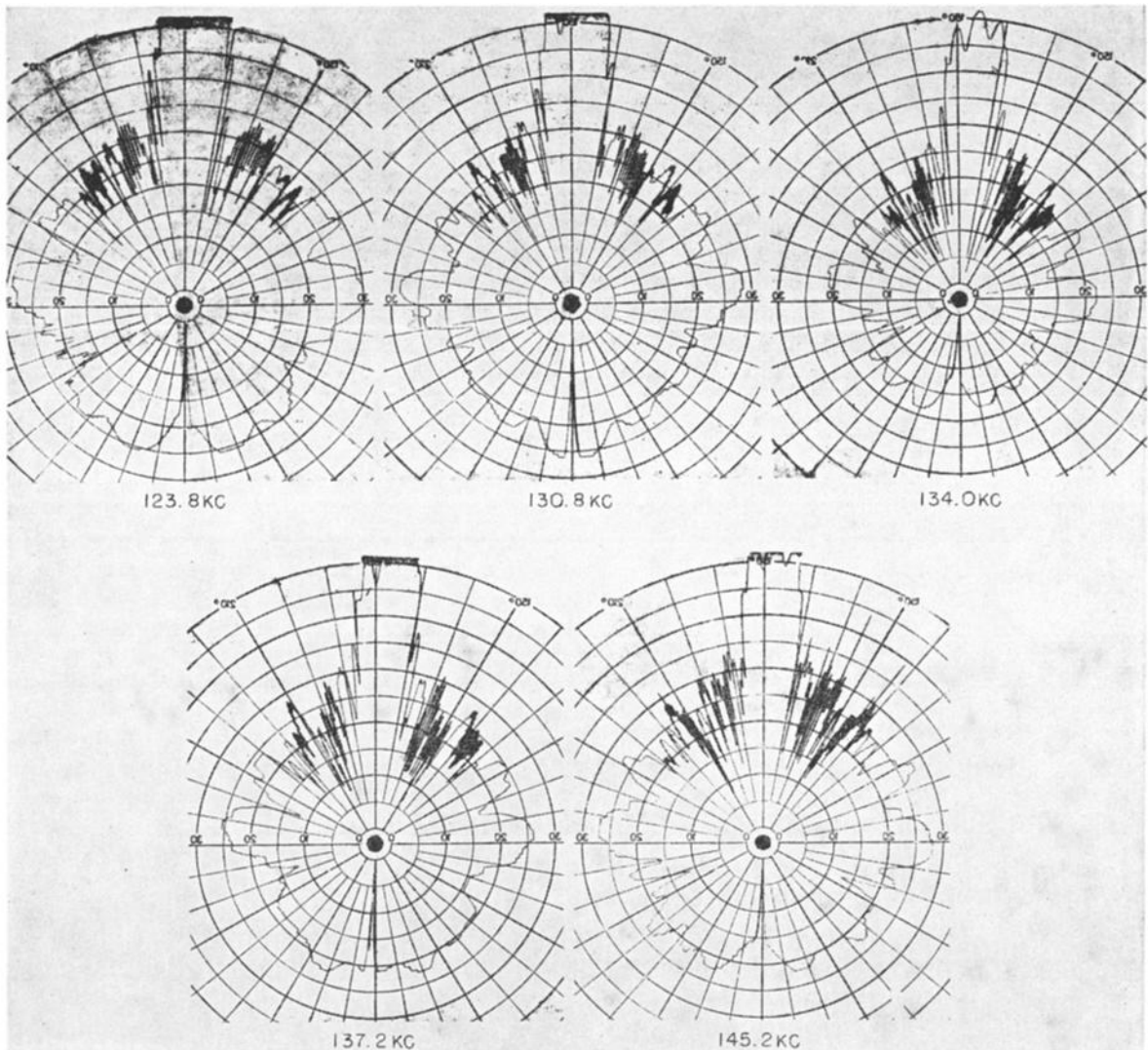

FIG. 13. The distribution in angle of acoustic energy scattered from a 5-in. diam solid aluminum sphere showing successive peaks and nulls in back-scattered signal. Pulse length: 500 μsec; radial scale: 5 db per division; angular scale: 10° per division; sound source at 0°.
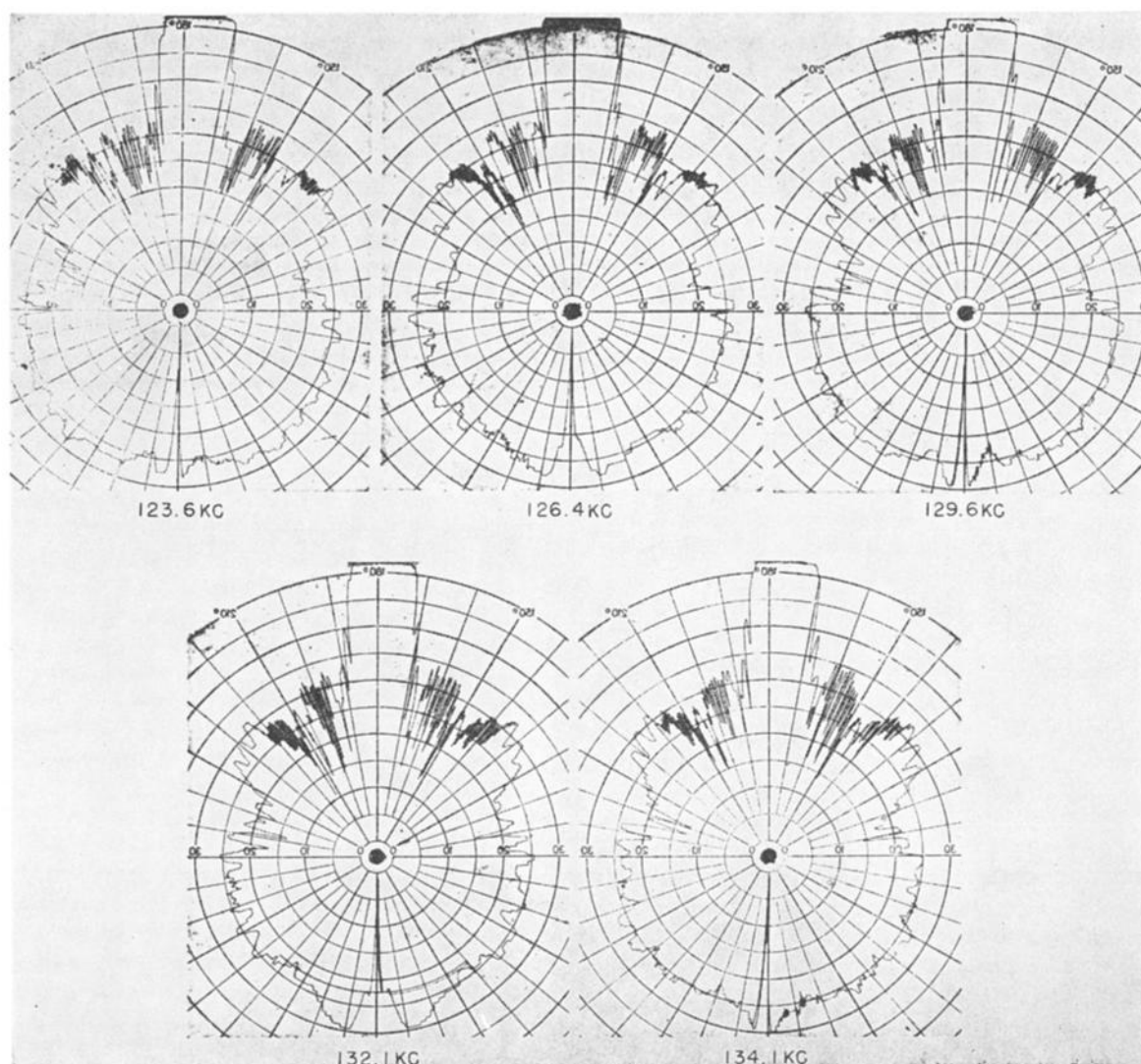
FIG. 14. The distribution in angle of acoustic energy scattered from a 5-in. diam solid brass sphere showing successive peaks and nulls in back-scattered signal. Pulse length: 500 μsec; radial scale: 5 db per division; angular scale: 10° per division; sound source at 0°.

destructive interference of the two signals. These fluctuations (moving from the backscattering point to the forward-scattering point) at first vary rapidly with change in angle since a small change in boom position produces a large phase difference in the direct path and the scattered path. As the boom approaches 180° the angular rate of fluctuation becomes slower as the rate of phase change for the two paths becomes less.

The angle at which interference from the direct path becomes significant depends on the pulse width. A short pulse is desirable because of the increased resolution between direct and scattered paths; however, for steady state conditions, the pulse must be at least twice the diameter of the sphere. The 500-μsec pulse has a range extent of 29 in. which is approximately four times the diameter of the largest sphere used and is a reasonable compromise between the two considerations. It is of

interest to note that in these measurements the recorded signal level for forward scattering with the sphere in place was never significantly greater than the direct path signal.

Figure 10 shows a series of scattering diagrams using the four aluminum spheres (7, 5, 3, and 1 in. in diam) at a frequency of 150 kc and using a pulse which has a range extent long compared to the sphere. These patterns cover a range of values of ka from 8.2 to 56. For the 7-in. diam sphere the boom was allowed to rotate twice with the sphere in position to show the repeatability of the pattern. For the 3- and 1-in. diam spheres the peak level of the forward scattered signal is off scale. The pattern for the 5-in. sphere does not have a second trace with the sphere removed.

Figure 11 shows scattering diagrams for equal values of ka, achieved by using two spheres at different fre-

quencies and using the long pulse condition. Figure 11(a) shows the diagrams for a 3-in. sphere at 50 kc superimposed on the plot for a 1-in. sphere at 150 kc, each having a value of *ka* of 8.2. The level of the two plots was adjusted to give best agreement in order to make a comparison. The variation in transducer beam pattern widths at the two frequencies causes a large difference in the patterns in the section between 150° and 210°. (The peak level of the direct signal is off scale.) In Fig. 11(b) a value of *ka* equal to 20 is achieved and in Fig. 11(c) *ka* is equal to 38. The patterns for the spheres removed are not shown. It can be seen that for the region not affected by direct path interference the patterns for each pair of spheres show rather good agreement.

Figure 12 shows the distribution in angle of scattered energy for the 5-in. diam brass sphere using a 500-μsec pulse and frequencies from 150 to 50 kc. At both 150 and 100 kc the scattering is essentially omnidirectional for the back 180°. The 150 and 100 kc patterns are not repeated with the sphere removed, and the peak level is off scale. A comparison with the patterns for the aluminum spheres indicates a considerable difference in the general positions of the lobes and nulls in the patterns.

The target strength data presented earlier indicated that the peaks and nulls in the backward-scattering targets as a function of frequency were very pronounced. Figure 13 is a group of patterns made at several successive peaks and nulls for the 5-in. diam aluminum sphere.

While the backscattered signal level changes vary rapidly, the general scattering pattern appears to remain fairly static. A similar series of patterns are shown for the 5-in. diam brass sphere in Fig. 14.

SUMMARY

In considering the scattering of acoustic plane waves by solid metal spheres in water, the spheres cannot be treated as rigid bodies since an appreciable amount of energy penetrates the surface and results in a more complicated echo structure for the scattered signals. The backscattered target strength of spheres for short pulses (and considering only the surface-reflected pulse) is essentially constant with frequency for large *ka*, and is slightly less than the theoretical value for rigid spheres, but for pulses which are long compared to the transit time across the sphere, the target strength fluctuates as much as 30 db for small changes in frequency. For short pulses the angular distribution of the scattered energy is fairly uniform over the back 180°, but this is not true for long pulses. In the forward direction, the interference between the scattered signals and the direct path signals result in rapid angular fluctuations in the composite signal level.

ACKNOWLEDGMENT